European Science Methodical Journal
ISSN (E): 2938-3641
Volume 2, Issue 3, March - 2024

SYNTHESIS OF NEW AROMATIC AZO-SCHIFF SULFONAMIDE DERIVATIVES AS CARBON STEEL ANTICORROSIVE IN 1 M HCL

Mohammed Abdulhussin Enad
Department of Pathological Analytics Science, College of Applied Medical Science, Shatrah University, Thi-Qar, 64001, Iraq.
Corresponding author e-mail: mohammed.76@utq.edu.iq

Abstract:

The synthetic sulfonamide derivative 4-((4-((4-chlorophenyl)imino)-2-hydroxypent-2-en-3-yl)diazenyl)benzenesulfonamide (HPDB) was studied using FT-IR, 13CNMR, and 1H NMR spectroscopy. Potentiometric polarization measurements were used to assess the inhibitory potential of the azo-azomethin molecule (HPDB). The presence of a physical adsorption process was corroborated by the thermodynamic features that were experimentally determined, and adsorption followed the "Langmuir" adsorption "isotherm". According to the electrochemical approach, raising the inhibitor concentration in 1M HCl solution enhanced the efficiency of the inhibition. It was also investigated how temperature affected the corrosiveness rate in the lack of and presence of these chemicals. For the dissolving process, the apparent activation energies, Arrhenius constant, enthalpies, and entropies were calculated and analyzed. The free energies and adsorption equilibrium constant were also found and discussed for the adsorption process. We gathered crucial knowledge regarding HPDB inhibitory behavior from the fundamental thermodynamic functions.

Keywords: Potentiometric, inhibitory, electrochemical.

Introduction

Society suffers from corrosion, which is a major global problem for metallic materials [1]. "Mild" steel (MS) is among the most significant materials for maritime engineering, oil, gas, heat exchangers, tanks, network pipes, and water utilities because of its excellent electrical, thermal, and mechanical properties. In brackish or drinkable waters, MS is prone to natural corrosion in the presence of hostile ions like chloride (Cl^-).Although hydrochloric acid (HCl) is a typical industrial cleaning, pickling, and descaling acid, it has harmful effects on metal surfaces due to its aggressive ions[2].On the other hand, many industrial synthesis processes frequently use acids and salts[3].Therefore, a suitable corrosion prevention strategy is needed to reduce different damages to the material and to preserve the economy. Corrosion inhibitors are essential as a result to prevent further harm to metallic components [4]. Numerous organic compou- nds with functional groups including -N=N, -CHO, R–OH, and NH2 were utilized as corrosion inhibitors in a variety of aqueous conditions. These compounds also had heteroatoms of nitrogen, sulfur, or oxygen [5]. A shielding layer is created on the metallic surface as a result

of these organic inhibitors adhering to it physically or chemically [6]. These two adsorption techniques provide a covering on the metal's surface that shields it from damaging ion bombardment [7]. Adsorption on a metallic surface causes organic inhibitors to react. Organic inhibitor molecules take the place of water molecules at metallic surfaces. When it comes to chemisorption, the anodic and cathodic processes are slowed down by the creation of a link between the metal and organic inhibitor, safeguarding the metal surface [8]. The effectiveness of these substances is heavily reliant on their capacity to form complexes with the metal since organic inhibitors work by adsorbing on the surface of the metal. Azo-azomethine Sulphonamides Derivatives are organic compounds that display great qualities that make them effective corrosion inhibitors, including the existence of heteroatoms with a single pair of electrons, numerous bonds (C=N, N=N), and aromatic rings [9]. Since the HCl environment is more corrosive than neutral or saline water settings, the chemicals used in this study were evaluated there rather than in those environments instead. Therefore, it is expected that the compounds investigated in this work will be acceptable corrosion inhibitors in less acidic conditions if they can tolerate the corrosiveness of HCl acid. In the investigation, various inhibitor concentrations and temperatures are taken into account.

2. EXPERIMENETAL

2.1. "Materials" and synthesis of HPDB

Original Content: Sourced from Fluka, our 4-chloroaniline and acetylaceton materials were top-notch. We also obtained HCl, NaNO2, Sodium carbonate, and sulphanilamide from the premium Sigma-Aldrich collection. No further purification was needed as we used analytical grade solvents, all thanks to Fluka. With precision in mind, we conducted our melting point measurements on the reliable Bauchi 510. As for our instrumentation, we meticulously recorded the compounds' solid-status FTIR spectra using KBr pellets and a Shimadzu FT-IR model 8400 S "Spectrophotometer".This covered a range of 4000 - 400 cm-1. Leveraging the power of a Brucker spectrophotometer (400 MHz), we investigated the 1HNMR and 13CNMR spectra with "DMSO-d_6" using TMS as an internal standard and our solvent. The chemical was created using the approach outlined in the literature by Erdem et al [10]. Initially, 10 mL of 2N HCl were used to dissolve 5 mmol of sulfanilamide (0.86 g), which was then agitated until a clear solution was produced. "Sodium nitrate" (7.50 mmol, 0.50 g) was then gradually while stirring was added and lowering the temperature of the solution to 0–5°C. Stirring continued for a further 45 minutes after the addition was finished. Separately, 30 mL of an aqueous Na2CO3 solution (20 mmol) was used to dissolve 0.5 g of acetylaceton (5 mmol), which was Afterwards, it was cooled in an ice bath to 0–5 °C. This combination was gradually added to the cold sulfanilamide diazonium salt solution. Another two hours were spent stirring at 0 to 5 degrees Celsius to maintain the pH at 6-7. The desired azo compound was obtained by recrystallizing the produced precipitate from ethanol after the precipitate had been manufactured. Through the use of thin-layer chromatography and an ethanol/chloroform (1:9) solvent system, the purity of the azo compound was evaluated. The fascinating and elaborate process of Schiff-base production, comprising a conventional condensation reaction, was

described. In this fascinating experiment, a balanced 1.0 mmol (0.28 g) of the alluring Azo compouned and the 1 mmol of the alluring aniline derivatives were smoothly dissolved in a negligible amount of methanol. We cautiously added a few drops of glacial acetic acid to intensify the process, and we let it to reflux for exciting periods of 5 to 12 hours. The product's thrilling result was then painstakingly investigated using TLC in an acetone/chloroform (7:3) mixture. In an exciting process, A freezing temperature was reached after cooling the reaction mixture., resulting in the formation of pure compounds. This intriguing precipitate was then carefully filtered and washed, using cold absolute methanol, before being left to dry in open air. A fascinating variety of synthetic preparations for azo-azomethine compounds are brilliantly encapsulated in Scheme 1

76% yield, M.P.209 ± 1℃. The chemical was created, and the FTIR spectra (Fig. 1) revealed the subsequent bands of absorption.: 1610 cm^{-1} (aromatic C=C), 3228-3305 cm^{-1} (NH_2), 3479 cm^{-1} "(O-H)", 1670 cm^{-1} "(C=N)" and 1482 cm^{-1} "(N=N)". Additionally, the SO_2 constituent may be seen in bands between 1317 cm^{-1} and 1153 cm^{-1}, which are the stretching vibrations of SO2 that are, respectively, asymmetrical and symmetric. [11,12].

Fig.2 shows ^{1}HNMR spectra (400 MHz, DMSO-d6) with 6.96 - 8.02 ppm (m, 4H, Ar-H) ,12.05 ppm (s, 1H, OH). 6.94 ppm (m, 2H, NH_2) and 5.91ppm (s, 6H, $2CH_3$). 163 ppm (C=N), 179 ppm (C-O), 117-145 ppm (aromatic ring) and 27 ppm (-CH_3) were found in 13CNMR spectra. Fig.3.

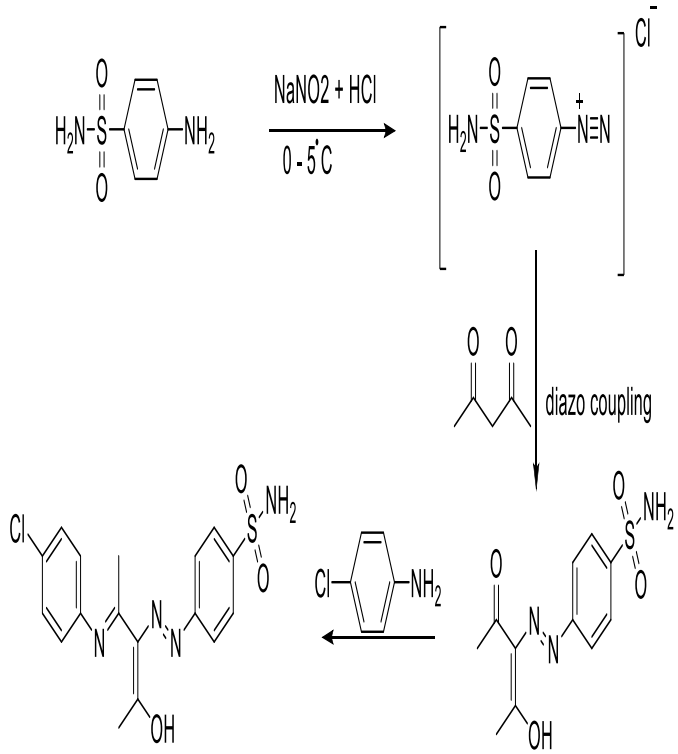

Scheme 1. Synthesis of (HPDB)

European Science Methodical Journal
ISSN (E): 2938-3641
Volume 2, Issue 3, March - 2024

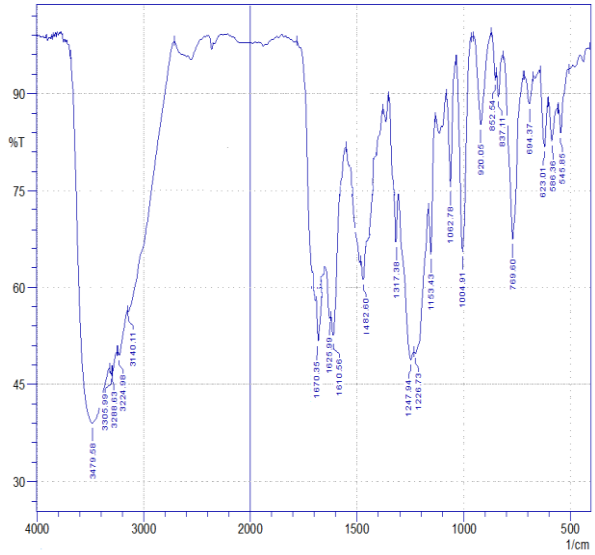

Fig. 1 .FT IR spectrum of (HPDB)

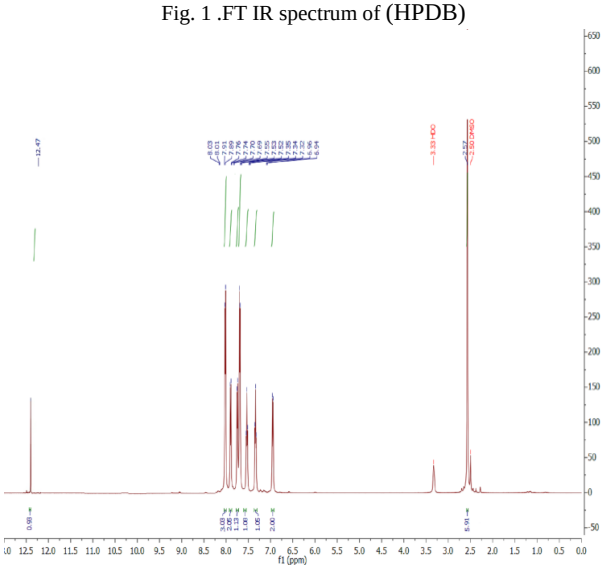

Figure 2. The (HPDB) 1HNMR "spectrum"

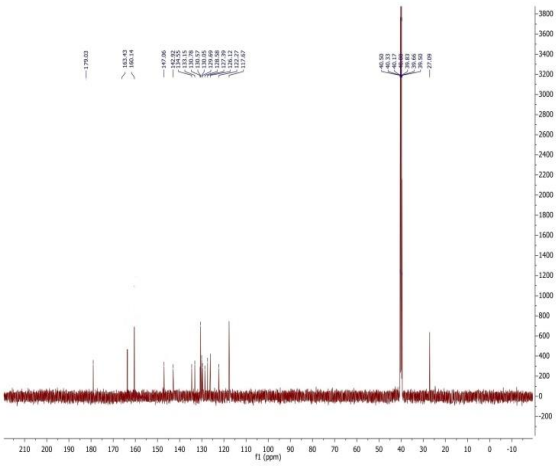

Figure 3: The (HPDB) ^{13}CNMR spectrum

European Science Methodical Journal
ISSN (E): 2938-3641
Volume 2, Issue 3, March - 2024

2.2. Spaceman preparation

The N-80 carbon steel sample that was employed in the experiment had a composition of 0.30% carbon, 0.050% phosphorus, 1.20% manganese, 0.060% sulfur, and iron as the final ingredient [13]. The mild steel surface was thoroughly cleansed with distilled water before each experimental test, washed with emery paper with a grit level of up to 1500, degreased with acetone, and then dried. Analytical grade 37% HCl was diluted to a concentration of 1M to create a hydrochloric acid solution. When the temperature fluctuated from 298, 308, and 318K and was set at ($5x10^{-4}$, $1x10^{-3}$, and $5x10^{-3}$M), The variety of inhibitor concentrations that were used in this investigation changed.

2.3. "Electrochemical" masurements

Electrochemical evaluations were made utilizing a Bank ELEIKTRONKIK INTELLGENT CONTROLS Model Mlab 200 with a three-electrode configuration comprised of a mild steel working electrode [WE], a platinum counter electrode [CE], and a reference electrode[RE] made of a saturated calomel with Ag/AgCl. A 30-minute stabilization period was allowed prior to all electrochemical measurements to provide an open circuit potential that is steady-state. It was possible to produce potentiodynamic polarization curves by rate of scan 1 mV s^{-1} over a potential fluctuate of [-250 to +250] mV (SCE)[14]. The temperatures of [298 K, 308 K, and 318 K] were utilized to run all the test solutions

3. RESULT AND DISCUTION

3.1. Measurements of the potentiodynamic polarization

Experiments were performed in 1 M HCl to comprehend how the resulting inhibitor, HPDB, affected carbon steel. Various doses of HPDB were used in potentiodynamic polarization studies at a range of temperatures between 298 and 318 K. Tafel slopes (β_a and β_c, respectively), for anodic and cathodic corrosion, as well as corrosion potential and current density, surface coverage (θ) and corrosion inhibitione efficacy (η %) were among experimental findings. Table 1 displays these outcomes. It is crucial to remember that the surface coverage and the percentage of inhibition have a strong correlation with I_{corr} values and may be calculated using tried-and-true techniques. The section of the Tafle plots was extrapolated in order to get the corrosion current density (I_{corr}). [15].

$$\%\,\eta = \left(\frac{I°corr - Icorr}{I°corr}\right) \times 100 \text{.....(1)}$$

$$\theta = \left(\frac{I°corr - Icorr}{I°corr}\right) \text{.....(2)}$$

the present study investigates the density of the corrosion currents, namely [I_{corr} and $I°_{corr}$] , in both "uninhibited" and "inhibited" states. The addition of hetero azo-azomethin group in HPDB serves as a potential inhibitor to reactive sites on mild steel surfaces. The experimental results demonstrate the density of the corrosion current reduces upon introduction of the inhibitor to aggressive media at constant temp. [16]. This study shows that a rise in inhibitor concentration corresponds due to a rise in I_{corr} concentration. Aside from that the increase in I_{corr} is caused by a rise in temperature. A approach of corrosion prevention is shown by the change in corrosion

potential (E_{corr}) of the inhibitors in the blank solutions. Corrosion potential data of the HPDB inhibitor showed no significant changes on either the cathode or anode side, indicating that the corrosion inhibitor is of the mixed type. This conclusion is the cathodic (βc) and anodic (βa) slope values provide support, which showed little difference compared to the blank values. Previous studies by Haiduc et al. showed that An inhibitor falls within the category of [anodic/cathodic] if the anodic/cathodic side offset E_{corr} is significantly bigger than 85 Mv [17]. In the course of our research, it was discovered that the shift in Ecorr values indicates that the HPDB inhibitor possesses the characteristics of a mixed-type inhibitor, with a range of less than 85 Mv. This observation provides a plausible explanation for the phenomenon that a decrease in temperature range resulted in lessening in inhibition efficacy, while an improvement in inhibitor concentration enhances inhibition effectiveness. As depicted in Figure 4, optimal conditions for HPDB in acidic media were determined to be 298 K and $5x10^{-3}$ M, corresponding to the lowest I_{corr} value of 4.4 Acm^2 and the highest IE% value of 85.62 Notably, the introduction of the corrosion inhibitor HPDB was found to significantly lower the rate of corrosion, with the lowest rate of corrosion (CR) being recorded at the highest inhibit. The equations 3 that follow were used to determine the corrosion rate:

C.R in (mpy) = $0.130 * I_{corr} * E.W / \rho$ …….. 3

E.W. : the metal's equivalent weight; ρ : the metal's density or alloy in (g/cm^3).

Table 1 : In 1M HCl with varying HPDB concentrations, carbon steel corrosion polarization includes were detected.

Tem. K	Inh. Con. M	E_{corr} mV	I_{corr} µA/Cm^2	β_a mv/Dec	β_c mv/Dec	IE%	θ	CR
298	blank	-461.1	30.6	296.9	-308.5	0	0	13.94
308		-464.1	35.6	362.0	-383.1	0	0	16.22
318		-441.7	39.2	328.1	-288.5	0	0	17.86
298	$5x10^{-4}$	-465.3	11.0	129.5	-127.1	64.12	0.641	5.01
308		-454.1	16.3	127.1	-129.1	54.21	0.542	7.43
318		-456.8	19.8	174.1	-167.8	49.44	0.494	9.02
298	$1x10^{-3}$	-466.7	6.9	92.1	-96.3	77.45	0.775	3.14
308		-450.4	9.6	135.1	-133.1	73.09	0.731	4.37
318		-449.9	11.6	110.7	-103.4	70.54	0.705	5.28
298	$5x10^{-3}$	-460.2	4.4	147.3	-161.6	85.62	0.856	2.05
308		-417.1	7.7	89.1	-88.8	78.37	0.784	3.51
318		-439.7	9.1	128.6	-120.8	76.79	0.768	4.15

European Science Methodical Journal
ISSN (E): 2938-3641
Volume 2, Issue 3, March - 2024

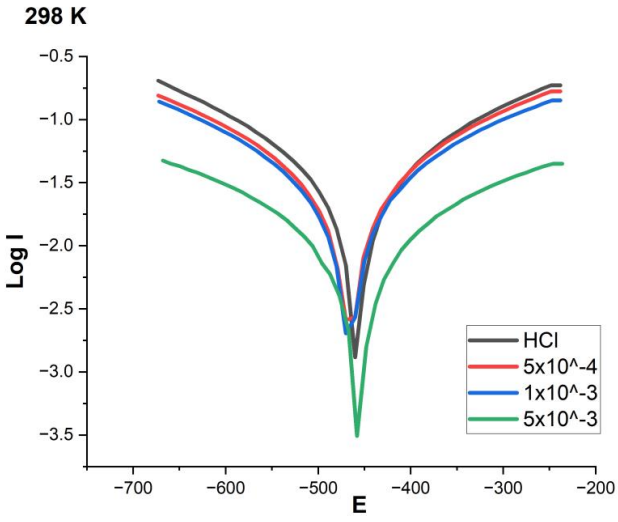

a

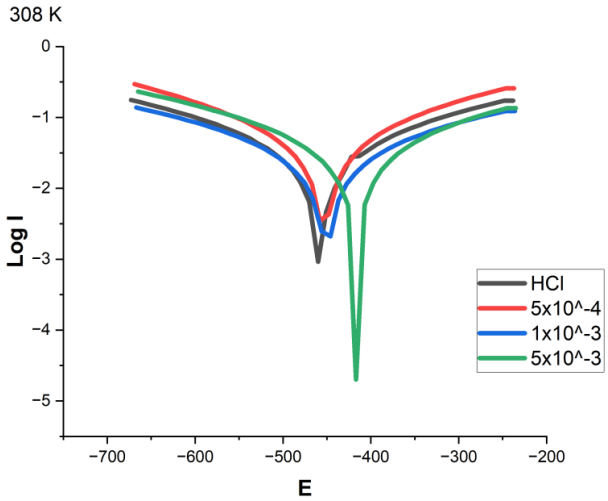

b

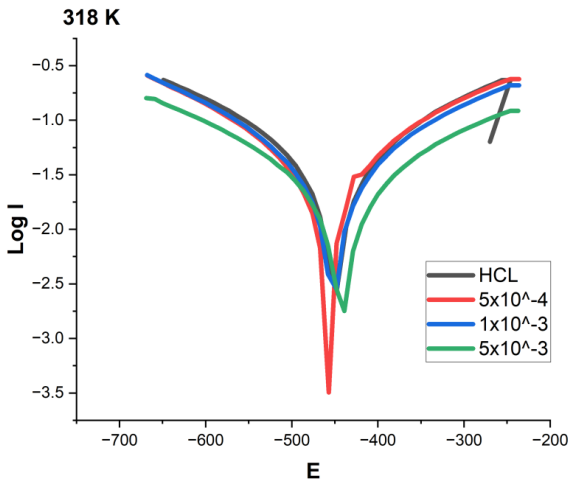

c

Fig. 4.Temperature-dependent potentiodyenamic "polarization" graphs about carbon steel in 1 M HCl with and without HPDB (a) 298 K, (b) 308 K, and (c) 318 K**.**

European Science Methodical Journal
ISSN (E): 2938-3641
Volume 2, Issue 3, March - 2024

3.2. Inhibitor Adsorption Iisotherm Model

The examination of adsorption isotherm and thermodynamic parameters plays a significant part in comprehending the inhibition regarding organic molecules' role in the corrosion process. It is logical to investigate the process by which these molecules adhere to a surface made of metal. However, the majority of organic corrosion inhibitors' effectiveness is typically correlated with their ability to adsorb at the [metal/solution] contact. Possibly, this phenomena analyzed through isotherms of adsorption, which can offer further insight into the mechanisme of "adsorption" such as the various of interactions between the steel and the inhibitory sector. In fact "corrosion" inhibitores can be adsorbed based on two different forms of interactions at the interface: the first; due to electrostatic interactions between charged molecules and the surface of the metal, physical adsorption (weak contacts)' the secod; wich electron sharing between inhibitors and iron d orbitals occurs during chemical adsorption. In the present investigation, the"Langmuir isotherm"of adsorption was employed as an explanation of nature that which adsorps of azoazomethine "inhibitors" on the exterior of steel by adjusting covering the surface (θ) values for various HPDB concenetrations, as outlined in eq.(3). [18]

$$\frac{C_{inh}}{\theta} = \frac{1}{K_{ads}} + C_{inh} \quad (3)$$

the adsorption equilibrium constant, denoted as K_{ads}, the coverage of surface, represented by[θ], and the concentration of the inhibitor, expressed as C_{inh}, are the variables of interest in this study. Figure 5 displays a linear relationship between C_{inh}/ θ and Cinh at varying temperatures. The intercept within the straight-lined with the y-axis determines the value of K_{ads} at various degrees of temperatures, accompanied by a "correlation" coefficient ($R2 \geq 0.999$) indicating high accuracy. Therefore, the inhibitor's adsorption on the surfaces of mild steel adheres to the Langmuire "adsorption isotherm" at all temperatures studied [19]. The chemical interaction's standard adsorption free energy change value is calculated using the equation below[20].

$$Kads = \frac{1}{55.5}\exp\left(-\frac{\Delta Gads}{RT}\right) \ldots\ldots\ldots\ldots\ldots\ldots (4)$$

where the water's molar concentration is [55.5]. The global gas constant is R, and T stands for the absolute temp. According to these calculations, "Gibbs" free energy fluctuation is normally inversely correlated with K_{ads}., and the higher the negative value of Gads, the more inhibitory molecules can be adsorbed. In addition, HPDB molecules are believed to be spontaneous.The mild steel surface was absorbed by the negative Gads value[21]. The Kads values in Table 2 also describe the extent of the combination of adsorbent and adsorbate. The Kads content decreases with increasing temperature as the bond between the mild steel and the inhibitor molecules weakens. In addition, the G_{ads} value has been used in many studies to distinguish between chemisorption and physisorption processes. This process is called

Chemisorption occurs when the G_{ads} value is greater than -40 kJ/mol, as electrons are shared that exists between the metal and the inhibitor. The "physisorption" process, This entails the interaction of the inhibitor's charged metal surface with electrostatic forces., is believed to be possible when G_{ads} is greater than -20 kJ/mol[22]. As seen in Table 2, the Gads information are between -31.2 and -32.2 kJ/mol. the adhesion of molecules of HPDB on metal surfaces is

European Science Methodical Journal
ISSN (E): 2938-3641
Volume 2, Issue 3, March - 2024

believed to involve the processes of physisorption and chemisorption. In addition, the following equation illustrates how the "Van't Hoff" relationship was used to determine the enthalpy change of adsorption[23].

$$\text{Log } K_{ads} = \frac{-\Delta Hads}{2.303\ RT} + \text{Cons} \quad \text{..... (5)}$$

Here K_{ads} is adsorption's equilibrium value and $H°_{ads}$ is the heat of adsorption. Plot the logarithm of K_{ads} against [1/T] to determine the standard enthalpy (Figure 6). gave a line segment with a slope of [$H°_{ads}$ / R] according to the equation.(5). The inhibitor molecules are adsorbed exothermically on the surface of metal is represented by a negative $H°_{ads}$ value[24]. A negative $H°_{ads}$ result showed that the EI (%) decreased with increasing temperature. The significant value of H°ads (-17.81 kJ/mol) could Describe the gradual decrease in HPDB efficiency of inhibition with raising the temperature. This behavior can be explained as follows: At higher temperatures, there was increased desorption of inhibitory compounds deposited on the surface of the mild steel. The entropy value $S°_{ads}$ was positive, meaning that as the amount of inhibitor increased, the formation of the coated film became more ordered, or the reactants' reversal order increased towards the synthesis of Activated "complex". The adsorption entropy S°ads of the inhibitor can be determined use the equation below [25].

"$\Delta G°_{ads}$" = "$\Delta H°_{ads} - T\ \Delta S°_{ads}$" ……(4)

Table 2 contains a list of the obtained $S°_{ads}$ values.

Table 2 : Temperature-dependent thermodynamic characteristics of the generated inhibitor following its adsorption on a carbon steel surface in 1 M HCl

Com	T	R^2	Log K_{ads}	$\Delta \breve{G}_{ads}$ KJ.mol^{-1}	$\Delta \breve{H}_{ads}$ KJ.mol^{-1}	$\Delta \breve{S}_{ads}$ KJ.mol^{-1}
HPDB	298	0.999	3.72	-31.206	-17.806	0.0449
	308	0.998	3.64	-31.748		0.0452
	318	0.999	3.53	-32.247		0.0459

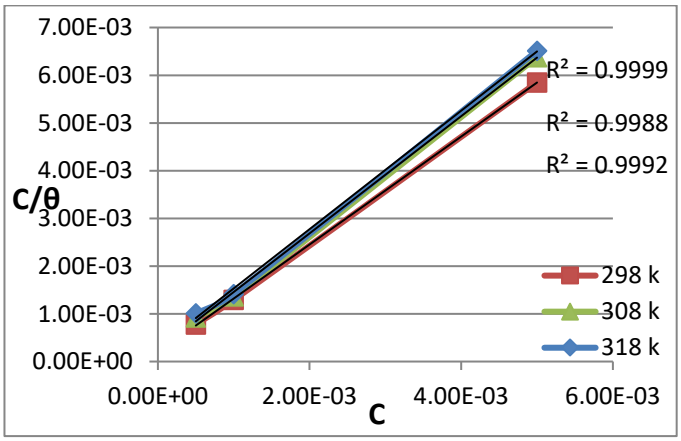

Fig. 5. An inhibitor HPDB adsorption model for the surface of carbon steel in 1 M HCl was created using the Langmuir isotherm.

.

European Science Methodical Journal
ISSN (E): 2938-3641
Volume 2, Issue 3, March - 2024

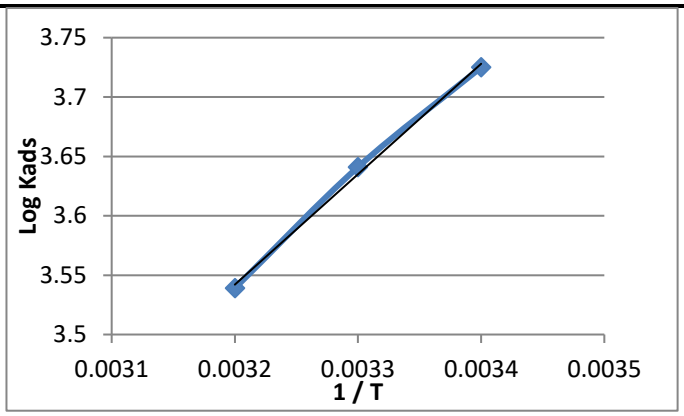

Fig. 6 : The correlation between [Log Kads and 1/T] for carbon steel in HCl solution of 1.0 M with various inhibitor quantities.

3.3 "Corrosion" kinetic and thermodynamic activation parameters

The influence temperature effects on corrosion rate of carbon steel in a 1.0 M HCl environment based on polarization curves in the range 298 to 318 K. The linear change in a measure of the corrosion current density's logarithm (i corr) as a consequence of the reciprocal in the presence of an inhibitor is depicted in Fig.6. of the temperature for a blank and in both situations. Examination for Explained by the activation parameters with and without inhibitor the mechanism of inhibitor "adsorption". The classic Arrhenius equation shown below may be used to compute the apparent activation energy (Ea). [26].

$$\text{Log (Icorr)} = \text{Log A} - \frac{\text{Ea}}{\text{RT}} \dots\dots\dots\dots\dots\dots (5)$$

Where R is the gas constant [Ea] is the corrosion reaction's activation energy (kJ mol^{-1}), In molecules cm-2 s-1, A is the preexponential factor., and T is the Kelvin-based absolute temperature.. Values for "(Ea)" were calculated using the linear "slopes" of the connection between [(log Icorr) and (1/T)] fig: 6. The "enthalpy" and entropy of the dissolution /passivation process were studied as activation parameters. [27]. The Formula for transition for the Arrhenius (equation (6)) can be used.

$$\log\left(\frac{\text{Icorr}}{\text{T}}\right) = \left[\text{Log}\left(\frac{\text{R}}{\text{hN}}\right) + \left(\frac{\Delta S*}{2.303\text{R}}\right)\right] - \frac{\Delta H*}{2.303\text{RT}} \dots.6$$

Where; The "temperature" is [T] in Kelvin terms, absolutely, The global gas constant is [R]. where [h] represents the Planck constant. [N] is Avogadroe's numbere, (ΔS*) is activeation entropy ΔH^* is the enthalpye of activation. The activation energy (Ea) is shown in Table 3 , and of Carbon stell In the absence as well as the presence of various variables concentrations of (HPDB). Every value for (Ea) exceeding the value in the blank. (12.44 kJ/mol), proving that (HPDB) retards the "Corrosion" response of Carbon stell [28]. A graph showing [log (Icorr/T) vs (1/ T)] (Equation 6) results in a linear relationship, as illustrated in Figure 7, wherein Table (3)'s predicted values for the activation thermodynamic parameters [ΔS* and ΔH*] and It has the following properties: [log(R/ Nh) + (ΔS*/ 2.303R)] as its intercept and a slope of [ΔH*/ 2.303R]. The comparison of energy that activates in the raw state and in the subsistence of an inhibitor makes it possible to predict a temperature's impact concerning braking efficiency.

European Science Methodical Journal
ISSN (E): 2938-3641
Volume 2, Issue 3, March - 2024

Radovici categorizes things in this way [29]. Conclusion: In our situation, the inhibitor has bonded to the steel surface via temperature-sensitive "electrostatic" bonds (weak bonds) [30]. Reduced correlation in braking efficiency as a temperature-dependent function with the shift of in the balance of adsorption and desorption. The positive enthalpy sign reflects the endothermic nature of the steel dissolution process. a rise in the entropy value as well signifies that as the chemicals afterwards become activated complexes in solution, there is a rise in disorder.

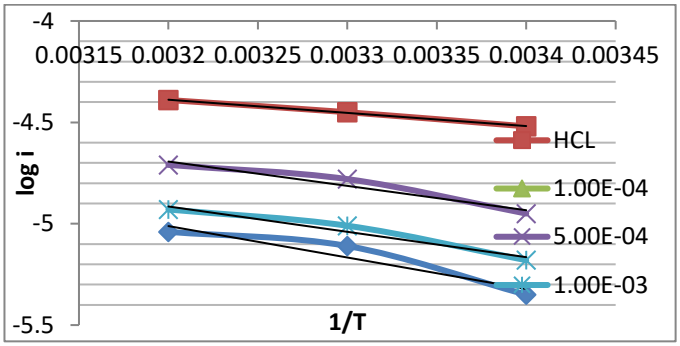

Figure 6. Plot [log (Icorr)] versus[(1/ T)] for carbon steel in 1M HCl with various doses of (HPDB) inhibitor.

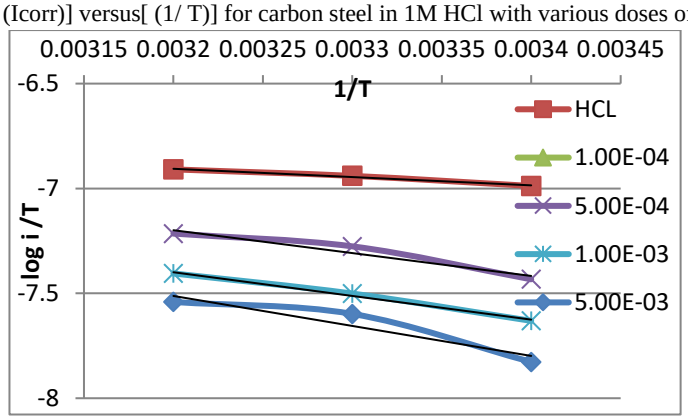

Figure 7 Plotlog (i_{corr}/T)] versus[(1/ T)] for carbon steel in 1.0M HCl with various doses of (HPDB) inhibitor...

Table 3 Corrosion kinetic characteristics at different temperatures of a carbon steel surface in 1 M HCl of the produced inhibitor..

Com	ΔH^{*} KJ.mol^{-1}	ΔS^{*} KJ.mol^{-1}K	E_a KJ.mol^{-1}
blank	7.56	-0.305	12.44
5x10^-4	20.87	-0.268	22.97
1x10^-3	21.11	-0.271	23.93
5x10^-3	27.38	-0.253	29.67

4. Suggestion of an inhibitory mechanism

The mechanisme of action of the inhibitors to preventing the (C.S) alloy from corroding in acidic solution (1M HCl) may be through absorbency of these inhibitions on the Carbon steel surface, forming an insulating layer that affects on the cathodic or anodic interaction or both of

them, and this Adsorption is influenced by the chemical constitution of these inhibitors in terms of the presence of heterogeneous atoms with high electronegativity such as (O, N, S) and the bond electrons (π) of aromatic rings through which the "inhibitor" adsorbs to the metal's surface., and these inhibitors are usually organic [31]. According to the results of the experimental results obtained from the various techniques used that were obtained , in 1.0 M HCl solution, the investigated organic dyes effectively prevent mild steel corrosion. previously published studies, the "mechanism" of inhibition The procedure with the tested organic molecules has been explored in detail Molecular Adsorption at the Metal/Solution Interface. The process of adsorption might take place physically, Chemically or a combination of the two adsorption types already discussed[32]. Physisorption: is a weak physical force of van der Waals adsorption or electrostatic interaction that occurs between the adsorbing surface and the adsorbed atoms or molecules or ions. The chlorine ion is first adsorbed on the external layer of the Carbon Steelalloy which carries a positive charge, as in the reaction (7), the molecules of the inhibitor are subsequently adsorbed during the electrostatic inter-action between the exterior of the negatively charged carbon Steel alloy ($FeCl^-$) and the protonization inhibitor molecule of the positively charged, and in this way, form a layer protection that prevents the alloy from disintegration (anodic reaction) according to the reaction (7 – 10).

$Fe + Cl \rightarrow [FeCl^-]_{ads}$ ……. 7

$[FeCl^-]_{ads} \rightarrow [FeCl^-]_{ads} + e^-$ ……...…8

$[FeCl^{1-}]_{ads} \rightarrow [FeCl^{1+}]_{ads} + e^-$ …..…..9

$[FeCl^{1+}]_{ads} \rightarrow Fe^{2+} + Cl^-$ …….10

When hydrogen ions compete with the inhibitory molecules for adsorption on the alloy surface. According to the reaction (11–13), this results in a slower reaction rate and releases the hydrogen gas (cathodic reaction). [33,34].

$Fe + H^+ \rightarrow [FeH^+]_{ads}$ …….. 11

$[FeH^+]_{ads} + e^- \rightarrow [FeH]_{ads}$ ……..……12

$[FeH]_{ads} + e^- + H^+ \rightarrow Fe^{2+} + H_2$ …….13

Additionally, the process of adsorbing inhibitor molecules entails replacing one or more of the water molecules that were previously The inhibitor molecules or the anions of the acid medium are adsorbed on the metal surface.

$Inh._{sol} + x\ H_2O_{ads} \rightarrow Inh_{ads} + x\ H_2O_{sol}$ …..14

where (x) denotes the water molecule count or size ratio that an organic inhibitor replaces with one. According to Equation (14), Possibly, the inhibitor molecules subsequently combine to produce metale inhibitor complexes with the freshly formed Fe^{2+}. Therefore, it makes sense to speculate that the presence of the chloride ion (Cl^-) on the steel surface may encourage the positive complex to bind to the surface via electrostatic interactions. [35].

$Fe^{2+} + Inh_{ads} \rightarrow [Fe – Inh]^{2+}_{ads}$ ……15

Chemisorption: is the formation of covalent or ionic bonds, coordinate bonds or a mixture thereof between the surface of the adsorbent and the adsorbed molecules, atoms or ions. Through a donor-acceptor contact (chemical adsorption), the electron pairs on the

heterogeneous oxygen, nitrogen, and sulfur atoms as well as the π electrons in the aromatic rings of the inhibitor molecules can adsorb. to adhere the particles to the surface, thus causing a chemical burn preventing substances from reaching the alloy surface, which reduces the corrosion rate [36,37].The studied inhibitory molecules are thought to be effective ligands because they can bind with metal ions to create coordination complexes[38]. Therefore, they can bind with the ions of Fe^{2+}, that develop on them create metal-inhibitor complexes [Fe2+ Inh.]ads on the steel surface, producing a block barrier for further resolution that corresponds with eq: 15.

5. CONCLUSION

For various concentrations, the inhibitory effectiveness was determined as a percentage of inhibitors in 1.0 M HCl as the corrosive medium at variousdegrees of temperatures by potentiodynamic polarization measurements. It has been observed that the percentage of inhibitory activity increases as increases inhibitor concentration at a fixed temperature and decreases when the temperature rises at a fixed concentration. The inhibitors tested functioned as mixed-type anodic-dominant inhibitors. Therefore, the high %IEs of achieved was interpreted as high organic molecule adsorption on mild steel surfaces with the tested inhibitors.. The Langmuir adsorption isotherm's prediction of this adsorption was proven to be accurate. HPDB adsorbs over the mild steel surface, and the fact that the Gibbs free energy of adsorption (Gads) is negative indicates the inhibitor compounds strongly contacted the mild steel surface.At 5x10-3 M concentration, the inhibition effectiveness was high (85.62%).

References

1. El-Haddad, M. N., & Fouda, A. E. A. S. (2021). Evaluation of curam drug as an ecofriendly corrosion inhibitor for protection of stainless steel-304 in hydrochloric acid solution: chemical, electrochemical, and surface morphology studies. Journal of the Chinese Chemical Society, 68(5), 826-836.
2. Verma, C., Ebenso, E. E., Bahadur, I., & Quraishi, M. A. (2018). An overview on plant extracts as environmental sustainable and green corrosion inhibitors for metals and alloys in aggressive corrosive media. Journal of molecular liquids, 266, 577-590.
3. Singh, P., Ebenso, E. E., Olasunkanmi, L. O., Obot, I. B., & Quraishi, M. A. (2016). Electrochemical, theoretical, and surface morphological studies of corrosion inhibition effect of green naphthyridine derivatives on mild steel in hydrochloric acid. The Journal of Physical Chemistry C, 120(6), 3408-3419.
4. Singh, M. B., Gabriel, B. I., Venkatraman, M. S., Cole, I. S., Moorthy, C. G., & Emmanuel, B. (2022). Theory of impedance for initial corrosion of metals under a thin electrolyte layer: a coupled charge transfer-diffusion model. Journal of Chemical Sciences, 134(1), 32.
5. Attar, T., Nouali, F., Kibou, Z., Benchadli, A., Messaoudi, B., Choukchou-Braham, E., & Choukchou-Braham, N. (2021). Corrosion inhibition, adsorption and thermodynamic properties of 2-aminopyridine derivatives on the corrosion of carbon steel in sulfuric acid solution. Journal of Chemical Sciences, 133, 1-10.

6. Mostfa, M. A., Gomaa, H., Othman, I. M., & Ali, G. A. (2021). Experimental and theoretical studies of a novel synthesized azopyrazole-benzenesulfonamide derivative as an efficient corrosion inhibitor for mild steel. Journal of the Iranian Chemical Society, 18, 1231-1241.
7. Nehra, B., Rulhania, S., Jaswal, S., Kumar, B., Singh, G., & Monga, V. (2020). Recent advancements in the development of bioactive pyrazoline derivatives. European Journal of Medicinal Chemistry, 205, 112666.
8. Abdallah, M., Fouda, A. S., Shama, S. A., & Afifi, E. A. (2008). Azodyes as corrosion inhibitors for dissolution of c-steel in hydrochloric acid solution. African Journal of Pure and Applied Chemistry, 2(9), 083-091.
9. Murulana, L. C., Kabanda, M. M., & Ebenso, E. E. (2015). Experimental and theoretical studies on the corrosion inhibition of mild steel by some sulphonamides in aqueous HCl. RSC advances, 5(36), 28743-28761.
10. Erdem, E., Sari, E. Y., Kilinçarslan, R., & Kabay, N. (2009). Synthesis and characterization of azo-linked Schiff bases and their nickel (II), copper (II), and zinc (II) complexes. Transition metal chemistry, 34, 167-174.
11. Jarrahpour, A. A., Motamedifar, M., Pakshir, K., Hadi, N., & Zarei, M. (2004). Synthesis of novel azo Schiff bases and their antibacterial and antifungal activities. Molecules, 9(10), 815-824.
12. Al-Atbi, H. S., Al-Assadi, I. J., Al-Salami, B. K., & Badr, S. Q. (2020). STUDY OF NEW AZO-AZOMETHINE DERIVATIVES OF SULFANILAMIDE: SYNTHESIS, CHARACTERIZATION, SPECTROSCOPIC, ANTIMICROBIAL, ANTIOXIDANT AND ANTICANCER ACTIVITY. Biochemical & Cellular Archives, 20.
13. ASTM International, "No Title," Stand. Pract. Prep. Cleaning, Eval. Corros. Test Specimens, vol. 90, no. G 1.
14. Salman, H. E., Balakit, A. A., & Allah, M. A. A. H. (2019, July). Study of the corrosion inhibitive effect and adsorption process of two azo-aldehydes on carbon steel in 1 M H2SO4. In IOP Conference Series: Materials Science and Engineering (Vol. 571, No. 1, p. 012078). IOP Publishing.
15. Boudjellal, F., Ouici, H. B., Guendouzi, A., Benali, O., & Sehmi, A. (2020). Experimental and theoretical approach to the corrosion inhibition of mild steel in acid medium by a newly synthesized pyrazole carbothioamide heterocycle. Journal of molecular structure, 1199, 127051.
16. Yusoff, M. H., Azmi, M. N., Hussin, M. H., Osman, H., Raja, P. B., Rahim, A. A., & Awang, K. (2020). An Electrochemical evaluation of synthesized coumarin-Azo dyes as potential corrosion inhibitors for mild steel in 1 M Hcl medium. International Journal of Electrochemical Science, 15(12), 11742-11756.
17. Rasheeda, K., Alamri, A. H., Krishnaprasad, P. A., Swathi, N. P., Alva, V. D., & Aljohani, T. A. (2022). Efficiency of a pyrimidine derivative for the corrosion inhibition of C1018 carbon steel in aqueous acidic medium: Experimental and theoretical approach. Colloids and Surfaces A: Physicochemical and Engineering Aspects, 642, 128631.

18. Sehmi, A., Ouici, H. B., Guendouzi, A., Ferhat, M., Benali, O., & Boudjellal, F. (2020). Corrosion inhibition of mild steel by newly synthesized pyrazole carboxamide derivatives in HCl acid medium: experimental and theoretical studies. Journal of the Electrochemical Society, 167(15), 155508.
19. Verma, C., Quraishi, M. A., Ebenso, E. E., Obot, I. B., & El Assyry, A. (2016). 3-Amino alkylated indoles as corrosion inhibitors for mild steel in 1M HCl: Experimental and theoretical studies. Journal of Molecular Liquids, 219, 647-660.
20. Radwan, A. B., Sliem, M. H., Yusuf, N. S., Alnuaimi, N. A., & Abdullah, A. M. (2019). Enhancing the corrosion resistance of reinforcing steel under aggressive operational conditions using behentrimonium chloride. Scientific reports, 9(1), 18115.
21. Durodola, S. S., Adekunle, A. S., Olasunkanmi, L. O., & Oyekunle, J. A. (2020). Inhibition of mild steel corrosion in acidic medium by extract of Spilanthes uliginosa leaves. Electroanalysis, 32(12), 2693-2702.
22. Dutta, A., Saha, S. K., Adhikari, U., Banerjee, P., & Sukul, D. (2017). Effect of substitution on corrosion inhibition properties of 2-(substituted phenyl) benzimidazole derivatives on mild steel in 1 M HCl solution: a combined experimental and theoretical approach. Corrosion Science, 123, 256-266.
23. Sliem, M. H., El Basiony, N. M., Zaki, E. G., Sharaf, M. A., & Abdullah, A. M. (2020). Corrosion inhibition of mild steel in sulfuric acid by a newly synthesized Schiff base: an electrochemical, DFT, and Monte Carlo simulation study. Electroanalysis, 32(12), 3145-3158.
24. Al-Joborry, N. M., & Kubba, R. M. (2020). Theoretical and Experimental Study for Corrosion Inhibition of Carbon Steel in Salty and Acidic Media by A New Derivative of Imidazolidine 4-One. Iraqi Journal of Science, 1842-1860.
25. Fawzy, A., & Toghan, A. (2021). Inhibition evaluation of chromotrope dyes for the corrosion of mild steel in an acidic environment: Thermodynamic and kinetic aspects. ACS omega, 6(5), 4051-4061.
26. Yadav, D. K., Maiti, B., & Quraishi, M. A. (2010). Electrochemical and quantum chemical studies of 3, 4-dihydropyrimidin-2 (1H)-ones as corrosion inhibitors for mild steel in hydrochloric acid solution. Corrosion Science, 52(11), 3586-3598.
27. Idouhli, R., Oukhrib, A., Khadiri, M., Zakir, O., Aityoub, A., Abouelfida, A., ... & Benyaich, A. (2021). Understanding the corrosion inhibition effectiveness using Senecio anteuphorbium L. fraction for steel in acidic media. Journal of Molecular Structure, 1228, 129478.
28. Olasunkanmi, L. O., Moloto, B. P., Obot, I. B., & Ebenso, E. E. (2018). Anticorrosion studies of some hydantoin derivatives for mild steel in 0.5 M HCl solution: Experimental, quantum chemical, Monte Carlo simulations and QSAR studies. Journal of Molecular Liquids, 252, 62-74.
29. Qiang, Y., Li, H., & Lan, X. (2020). Self-assembling anchored film basing on two tetrazole derivatives for application to protect copper in sulfuric acid environment. Journal of Materials Science & Technology, 52, 63-71.

30. Idouhli, R., Koumya, Y., Khadiri, M., Aityoub, A., Abouelfida, A., & Benyaich, A. (2019). Inhibitory effect of Senecio anteuphorbium as green corrosion inhibitor for S300 steel. International Journal of Industrial Chemistry, 10, 133-143.
31. Alkadir Aziz, I. A., Annon, I. A., Abdulkareem, M. H., Hanoon, M. M., Alkaabi, M. H., Shaker, L. M., ... & Takriff, M. S. (2021). Insights into corrosion inhibition behavior of a 5-mercapto-1, 2, 4-triazole derivative for mild steel in hydrochloric acid solution: experimental and DFT studies. Lubricants, 9(12), 122.
32. Fawzy, A., & Toghan, A. (2021). Inhibition evaluation of chromotrope dyes for the corrosion of mild steel in an acidic environment: Thermodynamic and kinetic aspects. ACS omega, 6(5), 4051-4061.
33. Qiang, Y., Zhang, S., Tan, B., & Chen, S. (2018). Evaluation of Ginkgo leaf extract as an eco-friendly corrosion inhibitor of X70 steel in HCl solution. Corrosion Science, 133, 6-16.
34. Qiang, Y., Zhang, S., Guo, L., Zheng, X., Xiang, B., & Chen, S. (2017). Experimental and theoretical studies of four allyl imidazolium-based ionic liquids as green inhibitors for copper corrosion in sulfuric acid. Corrosion Science, 119, 68-78.
35. Boudjellal, F., Ouici, H. B., Guendouzi, A., Benali, O., & Sehmi, A. (2020). Experimental and theoretical approach to the corrosion inhibition of mild steel in acid medium by a newly synthesized pyrazole carbothioamide heterocycle. Journal of molecular structure, 1199, 127051.
36. Ali, S. H., & Nabi, A. S. A. (2022). Synthesis, Identification And Inhibition Evaluation Of Azo Dyes For Corrosion of Carbon-Steel Alloy In Acidic Medium: Thermodynamic and Kinetic Aspects. Synthesis, 54(02).
37. Tanwer, S., & Shukla, S. K. (2022). Recent advances in the applicability of drugs as corrosion inhibitor on metal surface: A review. Current Research in Green and Sustainable Chemistry, 5, 100227.
38. Fu, L., Xiong, Y., Chen, S., & Long, Y. (2015). Trace copper ion detection by the suppressed decolorization of chromotrope 2R complex. Analytical Methods, 7(1), 266-270.